



## *In vitro* anti-melanogenic effects of chimeric compounds, 2-(substituted benzylidene)-1,3-indanedione derivatives with a $\beta$ -phenyl- $\alpha$ , $\beta$ -unsaturated dicarbonyl scaffold

Il Young Ryu<sup>a,1</sup>, Inkyu Choi<sup>a,1</sup>, Hee Jin Jung<sup>a,1</sup>, Sultan Ullah<sup>b,1</sup>, Heejeong Choi<sup>a</sup>, Md. Al-Amin<sup>a</sup>, Pusoon Chun<sup>c</sup>, Hyung Ryong Moon<sup>a,\*</sup>

<sup>a</sup> College of Pharmacy, Pusan National University, Busan 46241, South Korea

<sup>b</sup> Department of Molecular Medicine, The Scripps Research Institute, FL 33458, USA

<sup>c</sup> College of Pharmacy and Inje Institute of Pharmaceutical Sciences and Research, Inje University, Gimhae, Gyeongnam 50834, South Korea

### ARTICLE INFO

#### Keywords:

Tyrosinase inhibitor  
Indanedione  
 $\beta$ -phenyl- $\alpha$   
 $\beta$ -unsaturated dicarbonyl  
Anti-melanogenic effect  
Docking simulation  
Competitive inhibitor  
Chimeric compound  
Kojic acid

### ABSTRACT

Tyrosinase is considered a key contributor to melanogenesis, and safe, potent tyrosinase inhibitors are needed for medical and cosmetic purposes to treat skin hyperpigmentation and prevent fruit and vegetable browning. According to our accumulated SAR data on tyrosinase inhibitors, the  $\beta$ -phenyl- $\alpha$ , $\beta$ -unsaturated carbonyl scaffold in either *E* or *Z* configurations, can confer potent tyrosinase inhibitory activity. In this study, twelve indanedione derivatives were synthesized as chimeric compounds with a  $\beta$ -phenyl- $\alpha$ , $\beta$ -unsaturated dicarbonyl scaffold. Two of these derivatives, that is, compounds **2** and **3** (85% and 96% inhibition, respectively), at 50  $\mu$ M inhibited mushroom tyrosinase markedly more potently than kojic acid (49% inhibition). Docking studies predicted that compounds **2** and **3** both inhibited tyrosinase competitively, and these findings were supported by Lineweaver-Burk plots. In addition, both compounds inhibited tyrosinase activity and reduced melanin contents in B16F10 cells more than kojic acid without perceptible cytotoxicity. These results support the notion that chimeric compounds with the  $\beta$ -phenyl- $\alpha$ , $\beta$ -unsaturated dicarbonyl scaffold represent promising starting points for the development of potent tyrosinase inhibitors.

### 1. Introduction

Tyrosinases (also known as polyphenol oxidases) play key roles in mammalian melanogenesis and in the enzymatic browning of fruit or fungi [1]. The active site of tyrosinase contains two central copper(II) ions, which interact with histidine residues in the common mushroom (*Agaricus bisporus*) and human malignant melanoma tyrosinase [2,3]. Tyrosinases exist in various forms such as immature, mature and active forms in animals, plants and fungi [4]. Melanogenesis can be defined as the process that results in the formation of the dark macromolecular pigment melanin via a series of enzymatic and chemical reactions. Tyrosinase catalyzes different reactions in the melanin biosynthetic pathway in melanocytes such as the hydroxylation of L-tyrosine to L-DOPA and the oxidation of the L-DOPA to dopaquinone, which in man, is converted by a series of complex reactions involving cyclization and oxidative polymerizations to melanin [5,6].

Melanin is the pigment largely responsible for the color of skin and functionally acts as a barrier against ultraviolet radiation [7]. However, elevated levels of melanin in skin create aesthetic problems such as melasma, freckles, and age spots, and are also associated with the pathogenesis of melanoma [8–15], especially in the middle-aged and elderly [16]. Thus, research studies have focused on the development of tyrosinase inhibitors that prevent the production of excess melanin, and to date, have identified a large number of potent natural and synthetic tyrosinase inhibitors [9,17–27]. Some of these inhibitors such as arbutin, kojic acid and hydroquinone are being used as topical whitening or anti-hyperpigmentation agents [28,29]. However, although hydroquinone and kojic acid are used as whitening agents, they are also associated with an elevated risk of thyroid cancer [30] and with nephrotoxic [31], genotoxic [13], and cytotoxic (to melanocytes) effects [32]. Arbutin, another tyrosinase inhibitor, has fewer side effects but is hydrolyzed to D-glucose and hydroquinone by primary skin microflora

\* Corresponding author at: Laboratory of Medicinal Chemistry, College of Pharmacy, Pusan National University, Busan 46241, South Korea.

E-mail address: [mhr108@pusan.ac.kr](mailto:mhr108@pusan.ac.kr) (H.R. Moon).

<sup>1</sup> These authors (I.Y. Ryu, I. Choi, H.J. Jung, and S. Ullah) contributed equally to this work.

(*Staphylococcus epidermidis* and *Staphylococcus aureus*) [33].

Natural tyrosinase inhibitors are generally considered to be free of harmful side effects, but they have low potencies, poor stabilities, and are expensive, due to the lack of rich natural sources. Accordingly, scientists have focused on the development of low cost, potent synthetic tyrosinase inhibitors [34]. We have synthesized many tyrosinase inhibitors over the last decade [35–47], and as shown by Fig. 1, our studies have demonstrated that compounds containing the  $\beta$ -phenyl- $\alpha,\beta$ -unsaturated carbonyl scaffold often exhibit potent tyrosinase inhibitory activity. Initially, we synthesized compounds with the (*E*) scaffold geometry because they could be synthesized more easily and because they tend to be more stable than corresponding compounds with the (*Z*)-scaffold geometry.

In a previous study, to determine whether compounds with the (*Z*) geometry also exhibit potent tyrosinase inhibitory activities, we prepared a series of these compounds by condensing an appropriate benzaldehyde with 3-phenylisoxazol-5(*4H*)-one, which was easily prepared by reacting ethyl benzoylacetate with hydroxylamine·HCl in the presence of DABCO (1,4-diazabicyclo[2.2.2]octane) (Scheme 1) [48]. Due to steric hindrance by the phenyl group of 3-phenylisoxazol-5(*4H*)-one, compounds with a (*Z*)- $\beta$ -phenyl- $\alpha,\beta$ -unsaturated carbonyl scaffold were predominately obtained. A (*Z*)-derivative with a 2,4-dihydroxyl substituent on the  $\beta$ -phenyl ring of the scaffold more potently inhibited mushroom and B16F10 (a melanoma derived cell-line) tyrosinase than kojic acid, which suggested the  $\beta$ -phenyl- $\alpha,\beta$ -unsaturated carbonyl scaffold can confer potent tyrosinase inhibitory activity, regardless of scaffold geometry.

Based on our previous findings, we wondered whether chimeric compounds with a  $\beta$ -phenyl- $\alpha,\beta$ -unsaturated dicarbonyl scaffold (Fig. 2) also exhibit high tyrosinase inhibitory activity. In this study, we report the synthesis of 2-(substituted benzylidene)-1,3-indanedione derivatives and their abilities to inhibit mushroom tyrosinase and tyrosinase in B16F10 cells (a murine melanoma cell-line). In addition, we investigated their abilities to inhibit melanogenesis in B16F10 cells and their cytotoxic effects on this cell-line.

## 2. Results and discussions

### 2.1. Chemistry

Indanedione derivatives have been synthesized previously by many research groups [49–51]. As depicted in Scheme 2, 2-(substituted benzylidene)-1,3-indanedione derivatives with the  $\beta$ -phenyl- $\alpha,\beta$ -unsaturated dicarbonyl scaffold were synthesized. The derivatives 1 – 12 were easily prepared by condensation between 1*H* and indene-1,3 (*2H*)-dione and an appropriate benzaldehyde in 1 M HCl acetic acid solution. Twelve benzaldehydes including 2,4- and 3,4-dihydroxybenzaldehyde were used and condensation yields ranged from 43.1 to 99.8% (Table 1). The structures of the final compounds were confirmed by  $^1\text{H}$  and  $^{13}\text{C}$  NMR spectroscopy and high- and low-resolution mass spectroscopy.

### 2.2. Biology

#### 2.2.1. Mushroom tyrosinase inhibition assay

The inhibitory effects of the synthesized 2-(substituted benzylidene)-1,3-indanedione derivatives 1 – 12 on mushroom tyrosinase were investigated. Kojic acid, a well-known tyrosinase inhibitor, was used as the positive reference control. As depicted in Table 2, residual tyrosinase activities were determined after treating mushroom tyrosinase with each test compound at 50  $\mu\text{M}$ . Residual tyrosinase activity after treatment with kojic acid was 50%. Of 12 test compounds, compounds 2, 3, and 8 more potently inhibited tyrosinase than kojic acid. Compound 8 with a 2,4-dimethoxy substituent on the  $\beta$ -phenyl ring of the scaffold achieved a residual tyrosinase activity of 44%. According to our cumulative structure–activity relationship (SAR) data for tyrosinase inhibition, compounds with at least one hydroxyl group on the  $\beta$ -phenyl ring of the scaffold, such as 4-hydroxyl, 2,4-dihydroxyl, 3,4-dihydroxyl, 4-hydroxy-3-methoxyl, and 3-hydroxy-4-methoxyl, generally exhibit potent tyrosinase inhibitory activity. Therefore, it is notable that compound 8 showed stronger tyrosinase inhibition than kojic acid. Furthermore, our SAR data indicate that a 2,4-dihydroxyl substituent on the  $\beta$ -phenyl ring of the scaffold also markedly enhances tyrosinase inhibition. As was expected, compound 2 with the 2,4-dihydroxyl substituent reduced tyrosinase activity more than compound 8 or kojic acid (residual activity 14%). However, compound 3 with a 3,4-dihydroxyl

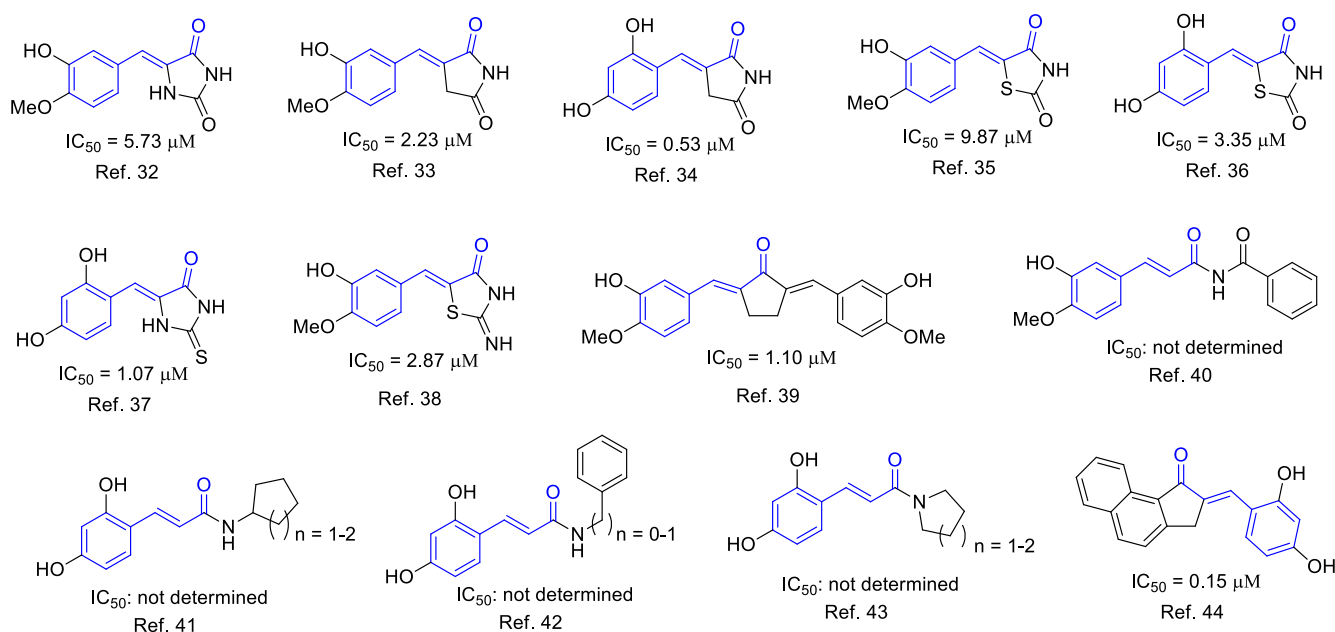
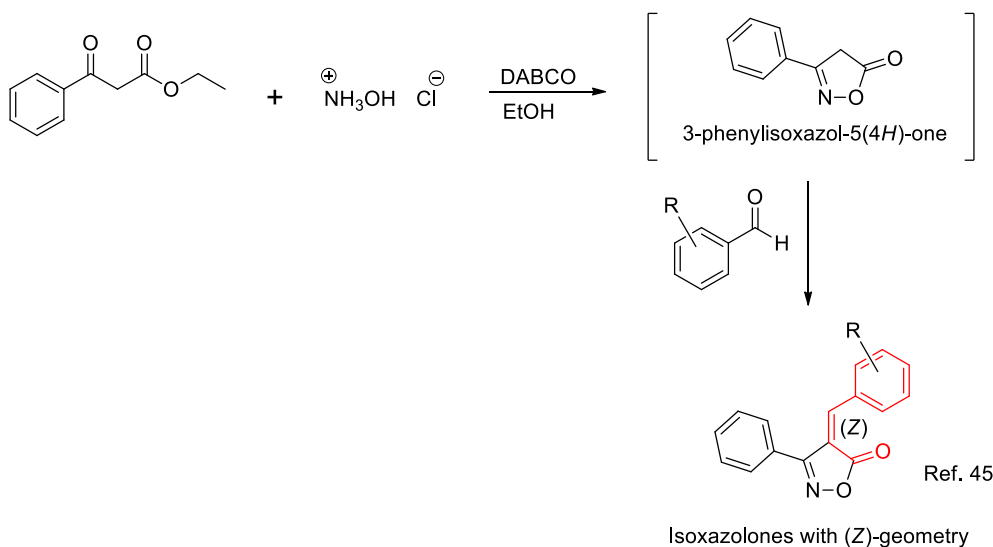
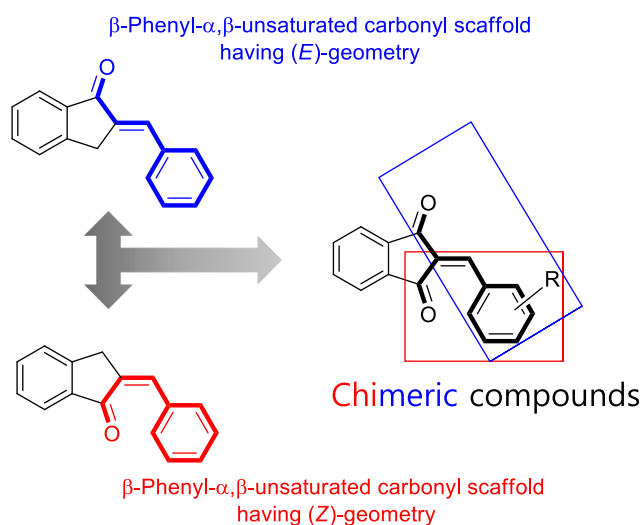


Fig. 1. Compounds containing the  $\beta$ -phenyl- $\alpha,\beta$ -unsaturated carbonyl scaffold that exhibit potent tyrosinase inhibitory activity.



**Scheme 1.** Schematic of the 3-phenylisoxazol-5(4H)-one based synthesis of compounds containing the (Z)- $\beta$ -phenyl- $\alpha,\beta$ -unsaturated carbonyl scaffold.



**Fig. 2.** Chimeric compounds, 2-benzylidene-indanediones with the  $\beta$ -phenyl- $\alpha,\beta$ -unsaturated dicarbonyl scaffold.

substituent on the  $\beta$ -phenyl ring had the greatest inhibitory effect and suppressed tyrosinase activity to only 4%. Log P values were obtained by ChemDraw Ultra 12.0 and the log P values of all synthesized compounds were better than the standard kojic acid.

Because compounds **2** and **3** inhibited tyrosinase more than kojic acid, we measured the  $IC_{50}$  values of these derivatives and of kojic acid using different concentrations. The  $IC_{50}$  value of kojic acid was  $50.10 \pm 2.63 \mu\text{M}$ , whereas those of **2** and **3** were  $32.15 \pm 0.63 \mu\text{M}$  and  $17.98 \pm 2.07 \mu\text{M}$ , respectively, that is, the 2 compounds inhibited tyrosinase 1.5- and 2.8-fold more than kojic acid (Table 2). Further studies are needed to determine whether compounds containing  $\beta$ -phenyl- $\alpha,\beta$ -unsaturated dicarbonyl have superior tyrosinase inhibitory effects compared to compounds containing  $\beta$ -phenyl- $\alpha,\beta$ -unsaturated carbonyl.

## 2.2.2. In silico studies

### 2.2.2.1. Binding pockets and enzyme-ligand interactions.

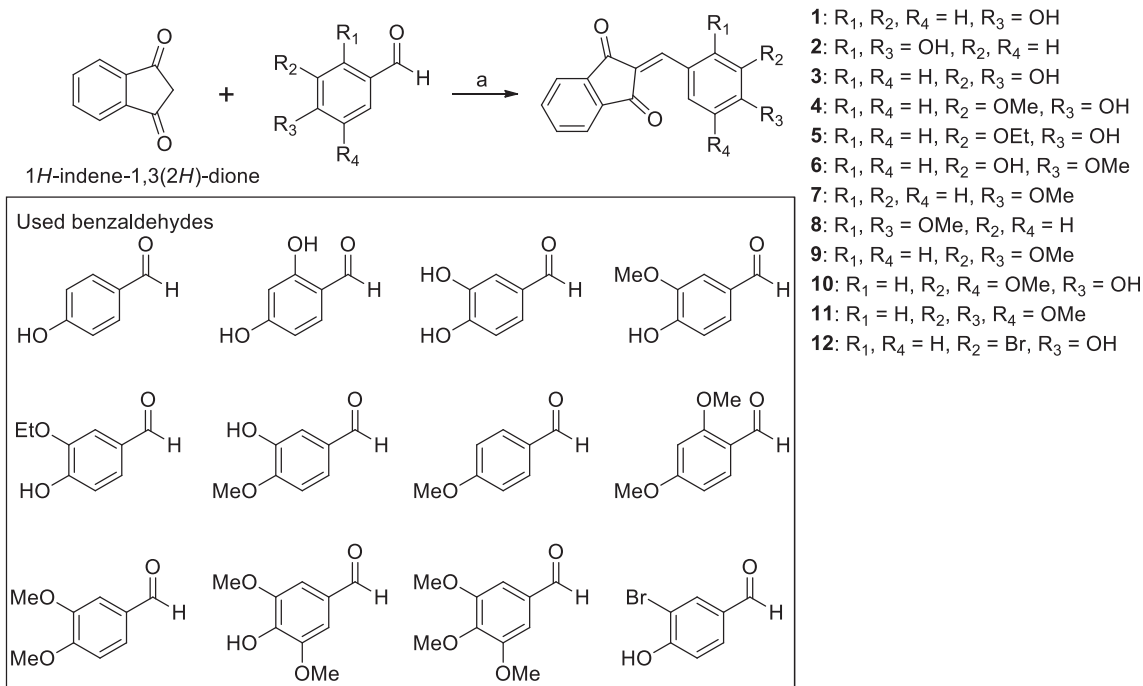
*In silico* docking simulation with mushroom tyrosinase was performed using Schrodinger Suite (release 2020–2) to predict the mode of action responsible for tyrosinase inhibition by compounds **2** and **3**. During the docking study,

we calculated binding energies of these ligands with mushroom tyrosinase and calculated the RMSD (root mean square deviation) values of hydrogen bonding and of interactions with the copper ions of tyrosinase. Binding interactions are shown in Fig. 3 in 2D and 3D format and in Fig. 5. As shown in Fig. 3b, compounds **2** and **3** occupied the same binding pocket as kojic acid. However, a detailed study of binding interactions (Fig. 3a) showed that compound **2** interacted more strongly with tyrosinase than compound **3** or kojic acid. Summarizing, kojic acid formed a hydrogen bond with Gly281 using its hydroxymethyl group and  $\pi$ - $\pi$  stacking interactions between the pyranone ring of kojic acid and the imidazole rings of tyrosinase His259 and His263. In addition, one non-classical hydrogen bond interacting with aromatic hydrogen (<https://www.schrodinger.com/training/videos/docking-receptor-grid-generation/hydrogen-bonds-aromatic-hydrogens-and-halogens>) was observed between the oxygen of the 3-hydroxyl pyranone group of kojic acid and the imidazolyl hydrogen of His259.

Compound **2** formed two hydrogen bonds and  $\pi$ - $\pi$  stacking,  $\pi$ -cation interactions, and hydrophilic interactions with various polar amino acid residues in the active site of tyrosinase. The hydroxyl groups of compound **2** at positions 2 and 4 on its phenyl ring formed two hydrogen bonds with Asn260 and Met280 of tyrosinase, respectively. In addition, the phenyl and the benzene rings of indanedione formed  $\pi$ - $\pi$  stacking and  $\pi$ -cation interactions with the His263 and Arg268 amino acid residues of tyrosinase, respectively. As shown in Fig. 5a, one non-classical hydrogen bond was also observed between the carbonyl group of compound **2** and the hydrogen at position 5 of the phenyl ring.

Compound **3** interacted with tyrosinase less than compound **2**, and notably, it did not form a classical hydrogen bond. Rather, it formed two  $\pi$ - $\pi$  stacking interactions between the indanedione benzene ring and the Hie244 (protonated His244) imidazole ring and between the phenyl ring of indanedione and the His259 imidazole ring. However, compound **3** did interact with a Cu ion, that is, the 4-hydroxyl group on the phenyl ring of **3** coordinated with this ion (Fig. 3a). One non-classical hydrogen bond was also observed between the indanedione carbonyl oxygen and the aromatic hydrogen of Phe264 (Fig. 5a). The docking simulations showed that compounds **2** and **3** bound to the active site of tyrosinase.

According to the docking simulation results in Fig. 3, compound **2** did not interact with copper ions, whereas compound **3** interacted with copper ions. To prove these results experimentally [52], the UV-visible spectra for compounds **2** and **3** were measured in the presence of mushroom tyrosinase with or without  $\text{CuSO}_4$  (0.125 mM) and the spectra are shown in Fig. 4. Regardless of the presence or absence of  $\text{CuSO}_4$ , the spectra of compound **2** were almost consistent ( $\lambda_{\text{max}} = 481$



**Scheme 2.** Synthesis of 2-(substituted benzylidene)-1,3-indanedione derivatives **1** – **12**. Reagents and conditions: (a) 1 M HCl in acetic acid, rt, 9 – 24 h, 43.1 – 99.8%.

**Table 1**

Synthetic yields and substitution patterns of 2-(substituted benzylidene)-1,3-

indanedione derivatives **1** – **12**.

Compound	R <sub>1</sub>	R <sub>2</sub>	R <sub>3</sub>	R <sub>4</sub>	Synthetic yield (%)
<b>1</b>	H	H	OH	H	86.8
<b>2</b>	OH	H	OH	H	43.1
<b>3</b>	H	OH	OH	H	75.7
<b>4</b>	H	OMe	OH	H	75.1
<b>5</b>	H	OEt	OH	H	99.8
<b>6</b>	H	OH	OMe	H	80.8
<b>7</b>	H	H	OMe	H	65.4
<b>8</b>	OMe	H	OMe	H	93.4
<b>9</b>	H	OMe	OMe	H	83.0
<b>10</b>	H	OMe	OH	OMe	79.2
<b>11</b>	H	OMe	OMe	OMe	57.7
<b>12</b>	H	Br	OH	H	75.1

nm). This result means that compound **2** does not interact with Cu<sup>2+</sup> in the active site of tyrosinase. However, in the case of compound **3**, in the absence of CuSO<sub>4</sub>, the spectrum showed a value of λ<sub>max</sub> at 502 nm, and the addition of excess CuSO<sub>4</sub> induced hypsochromic shift (λ<sub>max</sub> = 465 nm), implying that compound **3** interacts with Cu<sup>2+</sup> in the active site of tyrosinase.

**2.2.2.2. Docking scores and binding analysis.** Docking scores of compound **2**, compound **3**, and kojic acid with mushroom tyrosinase were determined using glide XP (Fig. 5b). Binding interactions were assessed by measuring atomic distances associated with binding interactions. In the case of kojic acid, the length of the hydrogen bond formed was 2.04 Å, whereas the aromatic hydrogen bond length was 3.33 Å (Fig. 5a). Kojic acid was also found to be located close to both copper ions. The

**Table 2**

Residual tyrosinase activities after treatment with 2-(substituted benzylidene)-1,3-indanedione derivatives **1** – **12**, and the IC<sub>50</sub> and Log P values.

Compound	Residual tyrosinase activity (%)	IC <sub>50</sub> (μM)	<sup>a</sup> Log P
Control	100	–	
<b>1</b>	82.71 ± 5.84	> 100	2.23
<b>2</b>	14.35 ± 1.52	32.15 ± 0.63	1.84
<b>3</b>	3.74 ± 1.68	17.98 ± 2.07	1.84
<b>4</b>	99.81 ± 14.08	> 100	2.11
<b>5</b>	99.26 ± 1.47	> 100	2.45
<b>6</b>	95.09 ± 2.28	> 100	2.11
<b>7</b>	67.50 ± 4.06	90.24 ± 2.91	2.50
<b>8</b>	44.32 ± 2.75	47.26 ± 1.52	2.37
<b>9</b>	66.53 ± 4.41	87.08 ± 2.67	2.37
<b>10</b>	99.95 ± 3.76	> 100	1.98
<b>11</b>	82.16 ± 5.31	> 100	2.24
<b>12</b>	72.47 ± 2.47	> 100	3.06
Kojic acid	50.01 ± 1.98	50.10 ± 2.63	–2.45

Tyrosinase inhibitory activity experiments were conducted at a concentration of 50 μM of derivatives and kojic acid. <sup>a</sup>Log P values were obtained by ChemDraw Ultra 12.0.

distances between copper 400 and 401 and the carbonyl oxygen of kojic acid were 3.16 Å and 2.68 Å, respectively. Based on these interactions, kojic acid achieved a docking score of –4.56 kcal/mole. Compound **2** achieved a higher docking score (–5.96 kcal/mol) than kojic acid or compound **3**, probably because it interacted with tyrosinase in more ways. Compound **2** formed two hydrogen bonds with lengths of 2.03 Å and 2.07 Å and one aromatic hydrogen bond of length 2.62 Å (Fig. 5). It also formed two π–π stacking interactions and interacted with Cu400 and Cu401 at distances of 4.56 and 3.46 Å, respectively. On the other hand, compound **3** did not form a hydrogen bond, but its 4-hydroxy on the phenyl ring interacted closely with Cu400 and Cu401 with bond distances of 2.58 and 2.30 Å, respectively. These results indicate that compound **3** bound deeper within the catalytic site of tyrosinase than compound **2** or kojic acid. Compound **3** also formed two π–π stacking interactions and an aromatic hydrogen bond of length 2.69 Å. The collective effects of these interactions led to stronger binding affinity



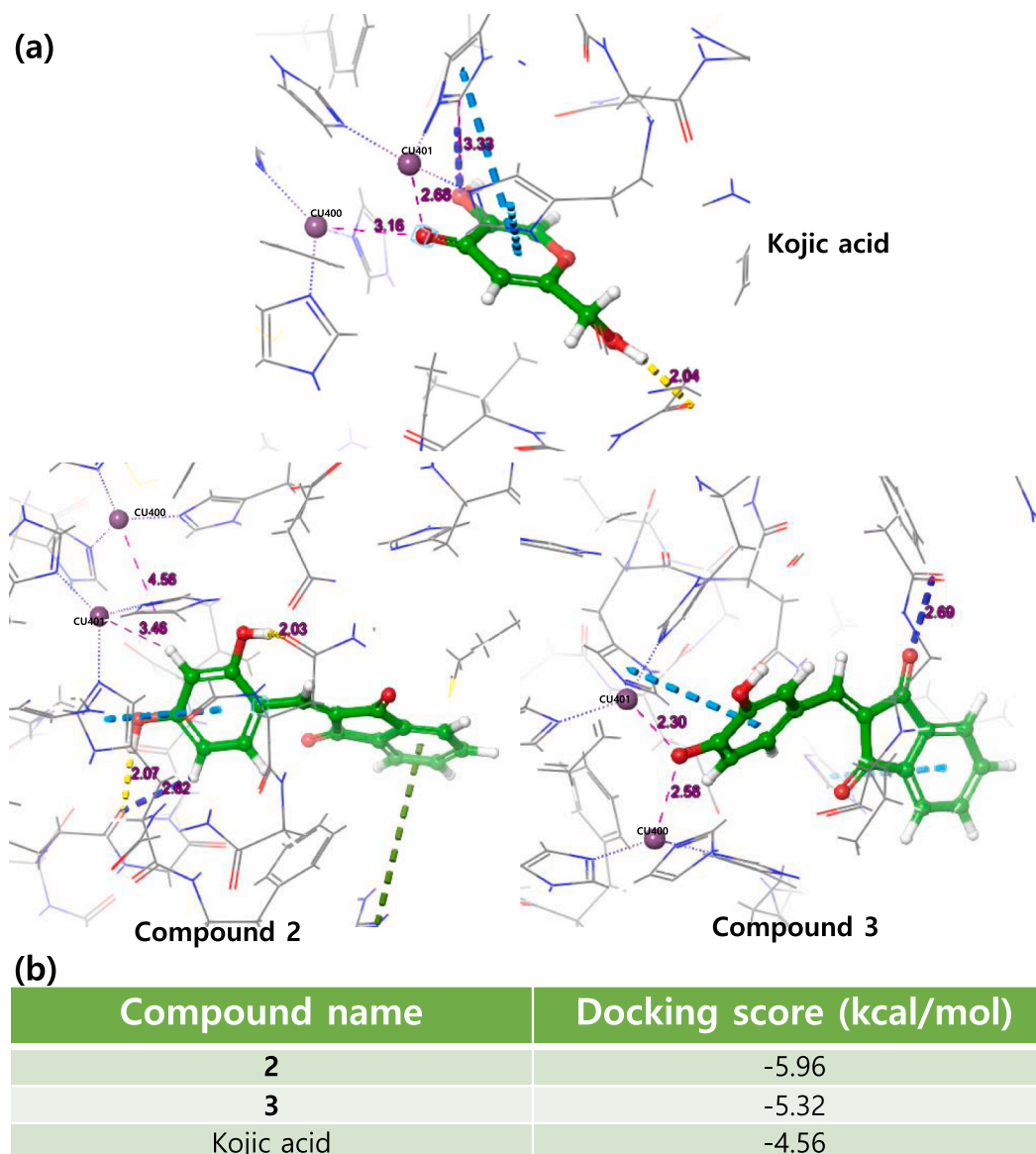


Fig. 5. Docking scores and binding analysis findings for interactions between mushroom tyrosinase (PDB ID = 2Y9X) and compound 2, compound 3, and kojic acid. Docking scores with tyrosinase were obtained using Maestro 12.4. Fig. 5a and 5b show bond lengths between ligands and amino acid residues, and docking scores, respectively.

concentrations increased and that  $K_M$  values gradually increased in a concentration-dependent manner. These results suggest that compounds 2 and 3 competitively inhibit tyrosinase by using the same binding pocket as natural tyrosinase substrates, as was predicted by docking simulation. The inhibitory kinetics (Table 3) showed the following: for 2;  $K_M = 4.00, 8.95,$  and  $22.10$  mM at  $7.5, 15,$  and  $30$   $\mu\text{M}$ , respectively; and for 3;  $K_M = 2.00, 3.07,$  and  $8.50$  mM, at  $7.5, 15,$  and  $30$   $\mu\text{M}$ , respectively.  $K_i$  values at concentrations of  $7.5, 15,$  and  $30$   $\mu\text{M}$  were  $2.82 \times 10^{-6}, 2.09 \times 10^{-6},$  and  $2.09 \times 10^{-6}$  M for 2, and  $4.70 \times 10^{-5}, 1.91 \times 10^{-5},$  and  $7.63 \times 10^{-6}$  M for 3, respectively. According to our previous data [53], kojic acid had  $3.16$  mM of  $K_M,$   $2.32 \times 10^{-4}$  M of  $K_i,$  and  $3.4 \times 10^{-2}$  mM/min of  $V_{\text{max}}$  at  $20$   $\mu\text{M}$ , respectively. Compounds 2 and 3 showed much lower  $K_i$  values than kojic acid.

#### 2.2.4. Cell study

**2.2.4.1. Cell viabilities.** Before performing *in vitro* experiments on murine B16F10 melanoma cells, we examined the effects of compounds 2 and 3 on B16F10 viability using an EZ-Cytox assay (Fig. 7). Compounds

2 and 3 did not show perceptible cytotoxicity up to a concentration of  $50$   $\mu\text{M}$ . Accordingly, further studies on the effects of 2 and 3 on tyrosinase inhibition and melanogenesis *in vitro* were conducted at concentrations of  $\leq 50$   $\mu\text{M}$ .

**2.2.4.2. Intracellular tyrosinase inhibition.** Initially, B16F10 cells were treated with  $5$   $\mu\text{M}$  of  $\alpha$ -melanocyte-stimulating hormone ( $\alpha$ -MSH) and  $200$   $\mu\text{M}$  of 3-isobutyl-1-methylxanthine (IBMX) for  $60$  h to enhance tyrosinase activity and then treated with compounds 2 or 3 ( $5, 10,$  or  $20$   $\mu\text{M}$ ), or kojic acid ( $20$   $\mu\text{M}$ ) for  $60$  h. Results are shown in Fig. 8. Treatment of cells with  $\alpha$ -MSH and IBMX enhanced intracellular tyrosinase activity by  $5.8$ -fold, and compounds 2 and 3 concentration-dependently reduced this increase (to  $2.7$ - and  $2.2$ -fold, respectively, at  $20$   $\mu\text{M}$ ). On the other hand, kojic acid at  $20$   $\mu\text{M}$  did not reduce  $\alpha$ -MSH and IBMX-induced increases in intracellular tyrosinase activity.

**2.2.4.3. Cellular melanin inhibition.** The effects of compounds 2 and 3 on melanin production were examined in B16F10 cells. As was performed for cellular tyrosinase activity experiments, cells were treated

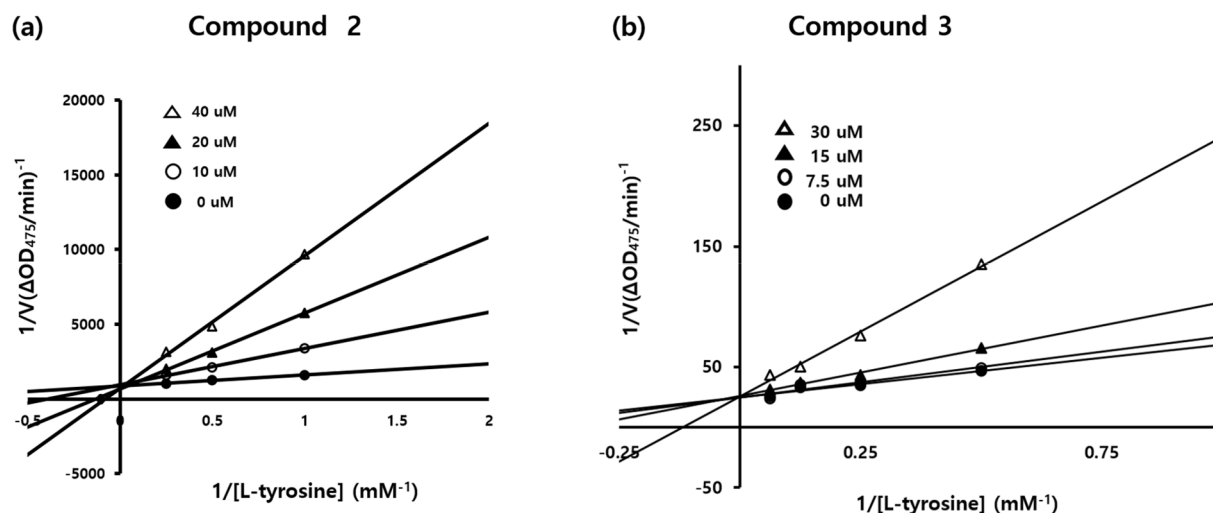


**Fig. 6.** Lineweaver-Burk plots of mushroom tyrosinase inhibition by compounds 2 and 3. For compound 2, concentrations of 0, 10, 20, or 40  $\mu\text{M}$  were used, and for compound 3, concentrations of 0, 7.5, 15, or 30  $\mu\text{M}$  were used. Each experiment was conducted in the presence of 0, 1, 2, or 4 mM of L-tyrosine for 2, and 0, 2, 4, 8, or 16 mM of L-tyrosine for 3.

**Table 3**  
Kinetic analysis of compounds 2 and 3.

Concentration ( $\mu\text{M}$ )	$V_{\text{max}}$ (mM/min)	$K_{\text{M}}$ (mM)	$K_{\text{i}}$ (M)
Compound 2 7.5	$3.3 \times 10^{-2}$	4.00	$2.82 \times 10^{-6}$
15	$3.3 \times 10^{-2}$	8.95	$2.09 \times 10^{-6}$
30	$3.3 \times 10^{-2}$	22.10	$1.56 \times 10^{-6}$
Compound 3 7.5	$4.0 \times 10^{-2}$	2.00	$4.70 \times 10^{-5}$
15	$4.0 \times 10^{-2}$	3.07	$1.91 \times 10^{-5}$
30	$4.0 \times 10^{-2}$	8.50	$7.63 \times 10^{-6}$

Data are mean values of  $1/V$  (inverse of the increase in absorbance at a wavelength of 475 nm per min ( $\Delta\text{OD}_{475}/\text{min}$ )), of three independent experiments conducted using different L-tyrosine concentrations. The Lineweaver-Burk plot equation is:  $1/V = 1/V_{\text{max}} + K_{\text{M}}/V_{\text{max}} \times 1/[S]$  and the modified Michaelis-Menten equation is  $1/V_{\text{max}} = (1 + [I]/K_{\text{i}}) \times 1/K_{\text{M}}$ , where  $V$  is the reaction rate,  $V_{\text{max}}$  is the maximum reaction rate,  $K_{\text{M}}$  is the Michaelis-Menten constant,  $[S]$  is substrate concentration,  $[I]$  is inhibitor concentration, and  $K_{\text{i}}$  is the inhibition constant.

with  $\alpha\text{-MSH}$  (5  $\mu\text{M}$ ) and IBMX (200  $\mu\text{M}$ ) before being treated with 2, 3, or kojic acid. The effects of 2 and 3 on melanin contents are shown in Fig. 9. Treatment with compound 2 did not reduce extracellular melanin contents in the concentration range 5–20  $\mu\text{M}$  (Fig. 9a), whereas it dose-dependently reduced intracellular melanin contents (Fig. 9b). At 20  $\mu\text{M}$ , compound 2 decreased intracellular melanin contents to the same extent as 20  $\mu\text{M}$  kojic acid. On the other hand, compound 3 dose-dependently and significantly reduced both extracellular and

intracellular melanin contents and showed much stronger anti-melanogenic effect than kojic acid (Fig. 9a and b). At 20  $\mu\text{M}$ , kojic acid did not reduce extracellular melanin levels.

These results suggest the inhibitory effects of compounds 2 and 3 on melanin production were due to tyrosinase inhibition. Numerous reports have determined only intracellular melanin levels to confirm the anti-melanogenic effects of the compounds, but we have examined both intracellular and extracellular melanin levels. Our results show that because the melanin synthesized by the B16F10 cells was released to the outside of the cells, the degree of inhibition of intracellular melanin levels influenced the extracellular melanin levels, and tyrosinase inhibitors had a greater effect on intracellular than extracellular melanin levels.

### 3. Conclusions

To examine whether chimeric compounds with the  $\beta$ -phenyl- $\alpha,\beta$ -unsaturated dicarbonyl scaffold plays an essential role in the inhibition of tyrosinase, twelve 2-(substituted benzylidene)-1,3-indanedione derivatives with the  $\beta$ -phenyl- $\alpha,\beta$ -unsaturated dicarbonyl scaffold were synthesized by Knoevenagel condensation. Mushroom tyrosinase inhibitory assays showed two 1,3-indanedione derivatives (compounds 2 and 3) with a 2,4- and 3,4- hydroxyls on the phenyl ring of the scaffold, respectively, inhibited tyrosinase significantly more than kojic acid. Docking studies on compounds 2 and 3 predicted that both bind more strongly to the active site of tyrosinase than kojic acid. Our kinetic study

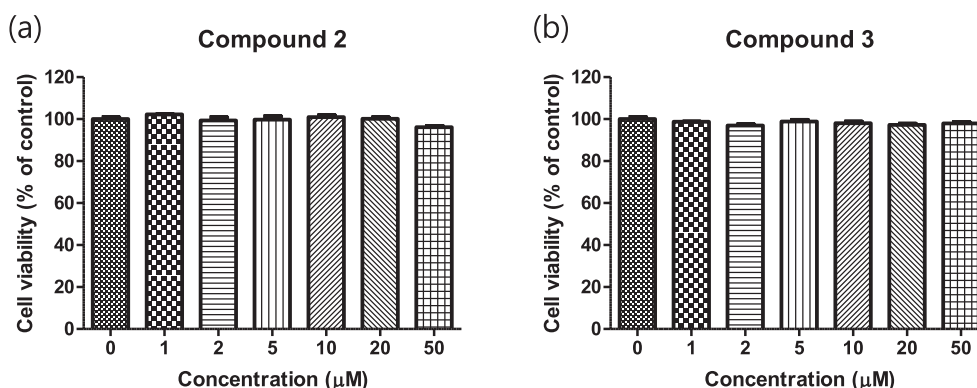


**Fig. 7.** Effects of compounds 2 and 3 on B16F10 cell viability. Cell viabilities were determined using EZ-Cytox solution at compound concentrations of 1 – 50  $\mu\text{M}$ .

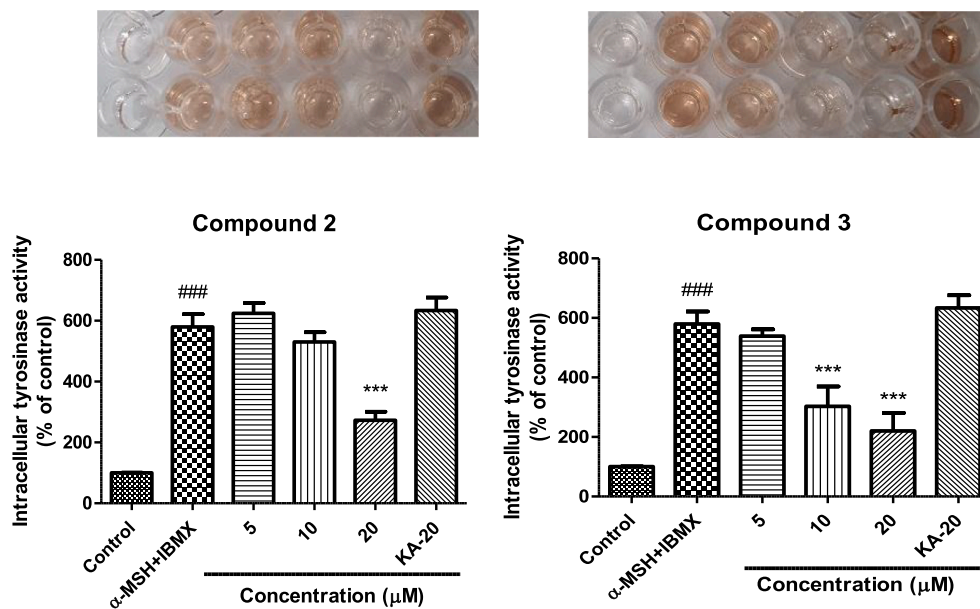


**Fig. 8.** Effects of compounds 2 and 3 on intracellular tyrosinase activity in B16F10 melanoma cells. Each experiment was carried out in triplicate and results are presented as means  $\pm$  SEMs. ### $p$  < 0.001, compared with the untreated controls; \*\*\* $p$  < 0.001, compared with  $\alpha$ -MSH and IBMX-treated cells.  $\alpha$ -MSH,  $\alpha$ -melanocyte-stimulating hormone; IBMX, 3-isobutyl-1-methylxanthine; KA, kojic acid.

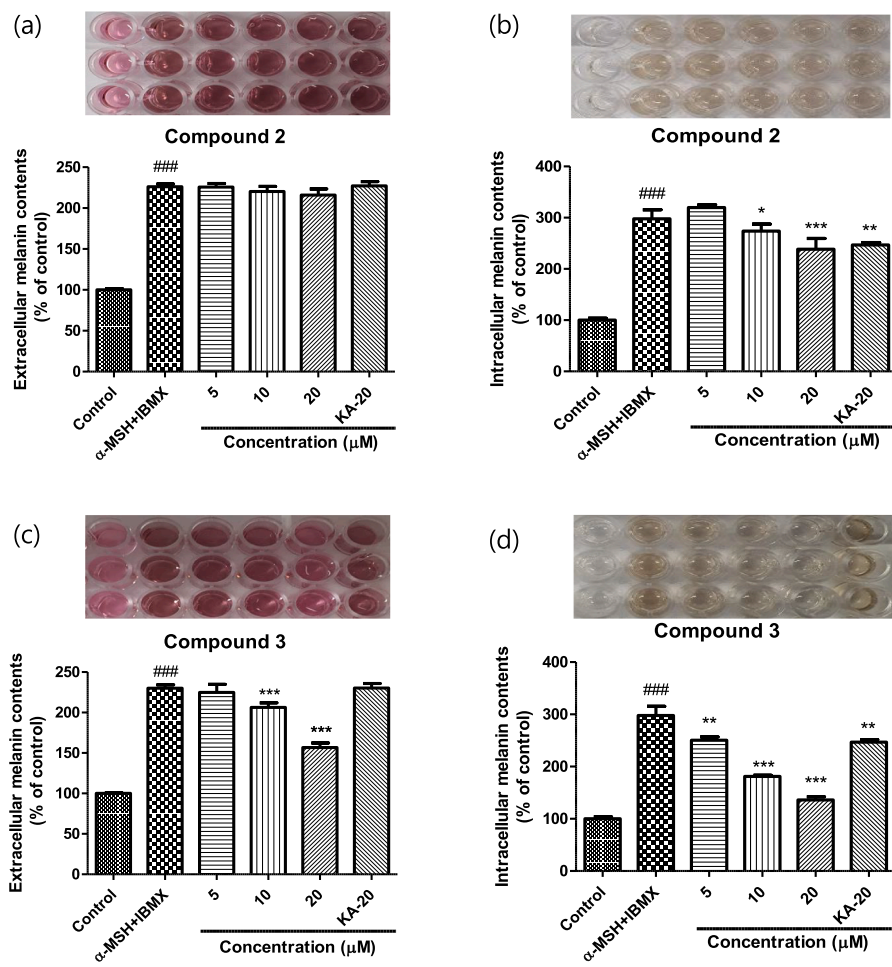


**Fig. 9.** Effects of compounds 2 and 3 on melanin production in B16F10 melanoma cells. Experiments were carried out in triplicate and results are presented as means  $\pm$  SEMs. (a) and (b) Extracellular and intracellular melanin contents of compound 2, respectively. (c) and (d) Extracellular and intracellular melanin contents of compound 3, respectively. ### $p$  < 0.001, compared with untreated controls; \* $p$  < 0.01, and \*\*\* $p$  < 0.001, compared with  $\alpha$ -MSH and IBMX-treated cells.  $\alpha$ -MSH,  $\alpha$ -melanocyte-stimulating hormone; IBMX, 3-isobutyl-1-methylxanthine; KA, kojic acid.

indicated that compounds **2** and **3** are a competitive tyrosinase inhibitor ( $V_{\max}$  remained constant regardless of concentration). *In vitro* experiments in B16F10 cells showed that compounds **2** and **3** dose-dependently inhibited intracellular melanin production and intracellular tyrosinase activity with no perceptible cytotoxicity. These results suggest that chimeric compounds with the  $\beta$ -phenyl- $\alpha,\beta$ -unsaturated dicarbonyl scaffold provide a basis for the design of potent tyrosinase inhibitors.

## 4. Experimental

### 4.1. Chemistry

#### 4.1.1. General methods

$^1\text{H}$  NMR and  $^{13}\text{C}$  NMR data were obtained using a Varian Unity INOVA 400 spectrometer or a Varian Unity AS500 spectrometer (Agilent Technologies, Santa Clara, CA, USA); DMSO- $d_6$  or  $\text{CDCl}_3$  were used as solvents. All chemical shifts were measured in parts per million (ppm) versus residual solvent or deuterated peaks ( $\delta_{\text{H}}$  7.24 and  $\delta_{\text{C}}$  77.0 for  $\text{CDCl}_3$ ,  $\delta_{\text{H}}$  2.50 and  $\delta_{\text{C}}$  39.7 for DMSO- $d_6$ ). Coupling constants are presented in hertz. The following abbreviations are used for  $^1\text{H}$  NMR: singlet (s), broad singlet (brs), doublet (d), doublet of doublets (dd), broad doublet (brd), triplet (t), broad triplet (brt), quartet (q) or multiplet (m). Low-resolution and high-resolution mass data were recorded on an Expression CMS (Advion Ithaca, NY, USA) in ESI positive and/or negative mode or an Agilent Accurate Mass Q-TOF liquid-chromatograph/mass spectrometer (Agilent, Santa Clara, CA, USA) in ESI positive mode, respectively. All reactions were conducted under nitrogen and monitored by thin-layer chromatography (TLC; Merck precoated 60F<sub>245</sub> plates). Solvents were distilled over Na/benzophenone or  $\text{CaH}_2$  before use.

**4.1.2. General procedure for the synthesis of 2-(substituted benzylidene)-1,3-indanedione derivatives 1 – 12:** A solution of 1,3-indanedione (100 mg, 0.68 mmol) and an appropriate benzaldehyde (1.0 – 1.1 equiv.) in 1 M HCl acetic acid (0.4 mL) was stirred at room temperature for 9 – 24 h. After adding water to the reaction mixture, the precipitate generated was filtered and washed with water and dichloromethane or hexane/dichloromethane (5:1 – 1:1) to give pure 2-(substituted benzylidene)-1,3-indanedione derivatives **1 – 12** in yields of 43.1 – 99.8% (Scheme 2).

**4.1.2.1. 2-(4-Hydroxybenzylidene)-1H-indene-1,3(2H)-dione (1).** Light brown solid, 86.8% yield.  $^1\text{H}$  NMR (400 MHz, DMSO- $d_6$ )  $\delta$  10.84 (brs, 1H, OH), 8.48 (d, 2H,  $J = 7.2$  Hz, 2'-H, 6'-H), 7.89 – 7.83 (m, 4H, 4-H, 5-H, 6-H, 7-H), 7.69 (s, 1H, vinylic H), 6.89 (d, 2H,  $J = 7.2$  Hz, 3'-H, 5'-H);  $^{13}\text{C}$  NMR (100 MHz, DMSO- $d_6$ )  $\delta$  190.6, 189.7, 164.0, 146.9, 142.3, 139.9, 138.3, 136.2, 136.0, 125.8, 125.3, 123.4, 123.4, 116.7; LRMS (ESI-)  $m/z$  249 (M-H) $^-$ ; HRMS (ESI+)  $m/z$   $\text{C}_{16}\text{H}_{11}\text{O}_3$  (M+H) $^+$  calcd. 251.0703, obsd. 251.0703.

**4.1.2.2. 2-(2,4-Dihydroxybenzylidene)-1H-indene-1,3(2H)-dione (2).** Brown solid, 43.1% yield.  $^1\text{H}$  NMR (400 MHz, DMSO- $d_6$ )  $\delta$  10.95 (s, 1H, OH), 10.81 (s, 1H, OH), 9.08 (d, 1H,  $J = 8.8$  Hz, 6'-H), 8.25 (s, 1H, vinylic H), 7.87 – 7.84 (m, 4H, 4-H, 5-H, 6-H, 7-H), 6.40 (d, 1H,  $J = 2.4$  Hz, 3'-H), 6.39 (dd, 1H,  $J = 8.8, 2.4$  Hz, 5'-H);  $^{13}\text{C}$  NMR (100 MHz, DMSO- $d_6$ )  $\delta$  191.3, 190.0, 166.7, 164.1, 142.1, 140.9, 139.7, 136.6, 135.9, 135.7, 123.1, 123.1, 113.8, 109.3, 102.5; LRMS (ESI-)  $m/z$  265 (M-H) $^-$ ; HRMS (ESI+)  $m/z$   $\text{C}_{16}\text{H}_{11}\text{O}_4$  (M+H) $^+$  calcd. 267.0652, obsd. 267.0649.

**4.1.2.3. 2-(3,4-Dihydroxybenzylidene)-1H-indene-1,3(2H)-dione (3).** Yellow solid, 75.7% yield.  $^1\text{H}$  NMR (400 MHz, DMSO- $d_6$ )  $\delta$  10.47 (s, 1H, OH), 9.54 (s, 1H, OH), 8.30 (s, 1H, 2'-H), 7.89 – 7.83 (m, 4H, 4-H, 5-H, 6-H, 7-H), 7.80 (d, 1H,  $J = 8.0$  Hz, 6'-H), 7.60 (s, 1H, vinylic H), 6.87 (d, 1H,  $J = 8.0$  Hz, 5'-H);  $^{13}\text{C}$  NMR (100 MHz, DMSO- $d_6$ )  $\delta$  190.7, 189.6, 153.3, 147.6, 146.0, 142.3, 139.8, 136.1, 135.9, 131.0, 125.8, 125.5, 123.3, 123.3, 121.3, 116.4; LRMS (ESI-)  $m/z$  265 (M-H) $^-$ ; HRMS (ESI+)  $m/z$   $\text{C}_{16}\text{H}_{11}\text{O}_4$  (M+H) $^+$  calcd. 267.0652, obsd. 267.0650.

**4.1.2.4. 2-(4-Hydroxy-3-methoxybenzylidene)-1H-indene-1,3(2H)-dione (4).** Yellow solid, 75.1% yield.  $^1\text{H}$  NMR (400 MHz, DMSO- $d_6$  +

$\text{CDCl}_3$ )  $\delta$  9.58 (brs, 1H, OH), 8.42 (s, 1H, 2'-H), 7.55 – 7.51 (m, 2H, 5-H, 6-H), 7.41 – 7.38 (m, 2H, 4-H, 7-H), 7.35 (s, 1H, vinylic H), 7.25 (d, 1H,  $J = 8.4$  Hz, 6'-H), 6.57 (d, 1H,  $J = 8.4$  Hz, 5'-H), 3.64 (s, 3H,  $\text{CH}_3$ );  $^{13}\text{C}$  NMR (100 MHz, DMSO- $d_6$  +  $\text{CDCl}_3$ )  $\delta$  190.6, 189.6, 153.2, 147.6, 147.6, 142.1, 139.6, 135.0, 134.8, 132.0, 125.6, 125.2, 122.7, 122.7, 116.2, 115.7, 55.9; LRMS (ESI-)  $m/z$  279 (M-H) $^-$ , 264 (M-H- $\text{CH}_3$ ) $^-$ ; HRMS (ESI+)  $m/z$   $\text{C}_{17}\text{H}_{13}\text{O}_4$  (M+H) $^+$  calcd. 281.0808, obsd. 281.0803.

**4.1.2.5. 2-(3-Ethoxy-4-hydroxybenzylidene)-1H-indene-1,3(2H)-dione (5).** Yellow solid, 99.8% yield.  $^1\text{H}$  NMR (500 MHz, DMSO- $d_6$ )  $\delta$  10.51 (brs, 1H, OH), 8.68 (s, 1H, 2'-H), 7.93 – 7.84 (m, 5H, 4-H, 5-H, 6-H, 7-H, 6'-H), 7.71 (s, 1H, vinylic H), 6.93 (d, 1H,  $J = 8.0$  Hz, 5'-H), 4.17 (q, 2H,  $J = 6.5$  Hz,  $\text{CH}_2\text{CH}_3$ ), 1.41 (t, 3H,  $J = 6.5$  Hz,  $\text{CH}_2\text{CH}_3$ );  $^{13}\text{C}$  NMR (100 MHz, DMSO- $d_6$ )  $\delta$  190.7, 189.9, 154.1, 147.6, 147.3, 142.3, 139.8, 136.2, 136.0, 132.4, 125.8, 125.6, 123.5, 123.3, 118.3, 116.4, 64.5, 15.3; LRMS (ESI-)  $m/z$  293 (M-H) $^-$ , 264 (M-H- $\text{C}_2\text{H}_5$ ) $^-$ ; HRMS (ESI+)  $m/z$   $\text{C}_{18}\text{H}_{15}\text{O}_4$  (M+H) $^+$  calcd. 295.0965, obsd. 295.0966.

**4.1.2.6. 2-(3-Hydroxy-4-methoxybenzylidene)-1H-indene-1,3(2H)-dione (6).** Yellow solid, 80.8% yield.  $^1\text{H}$  NMR (400 MHz,  $\text{CDCl}_3$ )  $\delta$  8.21 (s, 1H, 2'-H), 8.05 (d, 1H,  $J = 8.8$  Hz, 6'-H), 7.98 – 7.95 (m, 2H, 5-H, 6-H), 7.78 (s, 1H, vinylic H), 7.78 – 7.76 (m, 2H, 4-H, 7-H), 6.95 (d, 1H,  $J = 8.8$  Hz, 5'-H), 5.72 (s, 1H, OH), 3.98 (s, 3H,  $\text{CH}_3$ );  $^{13}\text{C}$  NMR (100 MHz,  $\text{CDCl}_3$ )  $\delta$  191.0, 189.6, 151.5, 147.4, 147.4, 145.6, 142.7, 135.3, 135.1, 129.7, 127.4, 127.3, 123.4, 123.3, 120.0, 110.6, 56.4; LRMS (ESI-)  $m/z$  279 (M-H) $^-$ , 264 (M-H- $\text{CH}_3$ ) $^-$ ; HRMS (ESI+)  $m/z$   $\text{C}_{17}\text{H}_{13}\text{O}_4$  (M+H) $^+$  calcd. 281.0808, obsd. 281.0809.

**4.1.2.7. 2-(4-Methoxybenzylidene)-1H-indene-1,3(2H)-dione (7).** Yellow solid, 65.4% yield.  $^1\text{H}$  NMR (500 MHz, DMSO- $d_6$ )  $\delta$  8.57 (d, 2H,  $J = 9.0$  Hz, 2'-H, 6'-H), 7.93 – 7.88 (m, 4H, 4-H, 5-H, 6-H, 7-H), 7.76 (s, 1H, vinylic H), 7.09 (d, 2H,  $J = 9.0$  Hz, 3'-H, 5'-H), 3.87 (s, 3H,  $\text{CH}_3$ );  $^{13}\text{C}$  NMR (100 MHz, DMSO- $d_6$ )  $\delta$  190.5, 189.6, 164.4, 146.4, 142.4, 139.9, 137.7, 136.3, 136.2, 126.9, 126.6, 123.5, 123.5, 115.1, 56.4; LRMS (ESI+)  $m/z$  265 (M+H) $^+$ ; LRMS (ESI-)  $m/z$  295 (M+MeOH-H) $^-$ , 248 (M-H- $\text{CH}_3$ ) $^-$ ; HRMS (ESI+)  $m/z$   $\text{C}_{17}\text{H}_{13}\text{O}_4$  (M+H) $^+$  calcd. 265.0859, obsd. 265.0858.

**4.1.2.8. 2-(2,4-Dimethoxybenzylidene)-1H-indene-1,3(2H)-dione (8).** Yellow solid, 93.4% yield.  $^1\text{H}$  NMR (500 MHz, DMSO- $d_6$ )  $\delta$  9.14 (d, 1H,  $J = 8.5$  Hz, 6'-H), 8.23 (s, 1H, vinylic H), 7.94 – 7.89 (m, 4H), 6.73 (d, 1H,  $J = 8.5$  Hz, 5'-H), 6.69 (s, 1H, 3'-H), 3.96 (s, 3H,  $\text{CH}_3$ ), 3.91 (s, 3H,  $\text{CH}_3$ );  $^{13}\text{C}$  NMR (100 MHz,  $\text{CDCl}_3$ )  $\delta$  191.4, 190.0, 166.6, 163.2, 142.5, 141.2, 140.2, 136.8, 135.0, 134.8, 125.7, 123.1, 123.1, 116.3, 105.8, 97.9, 56.0, 55.9; LRMS (ESI+)  $m/z$  349 (M+MeOH+Na) $^+$ , 317 (M+Na) $^+$ , 295 (M+H) $^+$ ; HRMS (ESI+)  $m/z$   $\text{C}_{18}\text{H}_{15}\text{O}_4$  (M+H) $^+$  calcd. 295.0965, obsd. 295.0965.

**4.1.2.9. 2-(3,4-Dimethoxybenzylidene)-1H-indene-1,3(2H)-dione (9).** Yellow solid, 83.0% yield.  $^1\text{H}$  NMR (500 MHz, DMSO- $d_6$ )  $\delta$  8.67 (s, 1H, 2'-H), 8.01 (d, 1H,  $J = 8.0$  Hz, 6'-H), 7.96 – 7.90 (m, 4H, 4-H, 5-H, 6-H, 7-H), 7.78 (s, 1H, vinylic H), 7.14 (d, 1H,  $J = 8.0$  Hz, 5'-H), 3.90 (s, 3H,  $\text{CH}_3$ ), 3.89 (s, 3H,  $\text{CH}_3$ );  $^{13}\text{C}$  NMR (150 MHz, DMSO- $d_6$ )  $\delta$  190.1, 189.4, 154.2, 148.8, 147.0, 142.2, 139.7, 135.7, 135.5, 131.5, 126.6, 126.5, 123.2, 123.0, 116.0, 111.5, 56.2, 56.0; LRMS (ESI-)  $m/z$  325 (M+MeOH-H) $^-$ , 293 (M-H) $^-$ ; HRMS (ESI+)  $m/z$   $\text{C}_{18}\text{H}_{15}\text{O}_4$  (M+H) $^+$  calcd. 295.0965, obsd. 295.0969.

**4.1.2.10. 2-(4-Hydroxy-3,5-dimethoxybenzylidene)-1H-indene-1,3(2H)-dione (10).** Orange solid, 79.2% yield.  $^1\text{H}$  NMR (400 MHz,  $\text{CDCl}_3$  + 2 drops of DMSO- $d_6$ )  $\delta$  8.68 (brs, 1H, OH), 7.72 (s, 2H, 2'-H, 6'-H), 7.65 – 7.62 (m, 2H, 5-H, 6-H), 7.50 – 7.48 (m, 2H, 4-H, 7-H), 7.45 (s, 1H, vinylic H), 3.70 (s, 6H, 2  $\times$   $\text{CH}_3$ );  $^{13}\text{C}$  NMR (100 MHz,  $\text{CDCl}_3$  + 2 drops of DMSO- $d_6$ )  $\delta$  190.7, 189.7, 148.0, 147.6, 142.4, 142.3, 139.7, 135.1, 134.9, 125.8, 124.4, 122.9, 122.9, 112.6, 56.4; LRMS (ESI-)  $m/z$  309 (M-H) $^-$ , 294 (M-H- $\text{CH}_3$ ) $^-$ ; HRMS (ESI+)  $m/z$   $\text{C}_{18}\text{H}_{15}\text{O}_5$  (M+H) $^+$  calcd. 311.0914, obsd. 311.0914.

**4.1.2.11. 2-(3,4,5-Trimethoxybenzylidene)-1H-indene-1,3(2H)-dione (11).** Orange solid, 57.7% yield.  $^1\text{H}$  NMR (500 MHz, DMSO- $d_6$ )  $\delta$  8.07 (s, 2H, 2'-H, 6'-H), 7.96 – 7.89 (m, 4H, 4-H, 5-H, 6-H, 7-H), 7.75 (s, 1H, vinylic H), 3.87 (s, 6H, 2  $\times$   $\text{CH}_3$ ), 3.79 (s, 3H,  $\text{CH}_3$ );  $^{13}\text{C}$  NMR (100 MHz, DMSO- $d_6$ )  $\delta$  190.1, 189.5, 153.1, 147.2, 143.1, 142.6, 140.0, 136.1,

136.0, 128.8, 128.2, 123.6, 123.4, 112.6, 60.9, 56.6; LRMS (ESI +)  $m/z$  379 (M + MeOH + Na)<sup>+</sup>, 347 (M + Na)<sup>+</sup>, 325 (M + H)<sup>+</sup>; HRMS (ESI +)  $m/z$  C<sub>19</sub>H<sub>17</sub>O<sub>5</sub> (M + H)<sup>+</sup> calcd. 325.1071, obsd. 325.1075.

4.1.2.12. 2-(3-Bromo-4-hydroxybenzylidene)-1H-indene-1,3(2H)-dione (**12**). Orange solid, 75.1% yield. <sup>1</sup>H NMR (400 MHz, DMSO-*d*<sub>6</sub>) δ 11.68 (s, 1H, OH), 9.06 (d, 1H, *J* = 2.0 Hz, 2'-H), 8.26 (dd, 1H, *J* = 8.8, 2.0 Hz, 6'-H), 7.94 – 7.85 (m, 4H, 4-H, 5-H, 6-H, 7-H), 7.68 (s, 1H, vinylic H), 7.04 (d, 1H, *J* = 8.8 Hz, 5'-H); <sup>13</sup>C NMR (100 MHz, DMSO-*d*<sub>6</sub>) δ 190.3, 189.8, 159.9, 145.3, 142.4, 140.0, 139.6, 137.4, 136.4, 136.3, 127.2, 126.6, 123.6, 123.5, 117.0, 110.5; LRMS (ESI-)  $m/z$  329 (M-H)<sup>-</sup>, 327 (M-2-H)<sup>-</sup>.

## 4.2. Biology

### 4.2.1. Mushroom tyrosinase inhibition assay of compounds 1–12 and kojic acid

A standard procedure was used to determine the mushroom tyrosinase inhibitory activities of the 12 test compounds, with some modification [54]. Two hundred μL of a mixture consisting of 20 μL of tyrosinase solution, 170 μL of substrate solution (14.7 mM phosphate buffer, and 293 μL L-tyrosine solution), and 10 μL of a test compound (1–12, final concentration: 50 μM) was placed in the wells of a 96 well plate. The plates were incubated at 37 °C for 30 min and optical densities were measured using a microplate reader (VersaMax™) at 450 nm. Kojic acid (50 μM) was used as the positive control. Experiments were repeated independently three times. The following formula was used to calculate tyrosinase inhibition.

$$\% \text{Inhibition} = [1 - (A/B)] \times 100$$

A represents test compound absorbance and B the absorbance of the untreated control.

### 4.2.2. In silico docking simulations of compound 2, compound 3, and kojic acid with tyrosinase

Schrodinger Suite (2020–2) was used for the *in silico* docking simulation studies. The three-dimensional (3D) structure of mushroom tyrosinase (*Agaricus bisporus*) (PDB ID: 2Y9X) was imported from the Protein Data Bank (PDB), and the protein structure of tyrosinase was prepared using the protein preparation wizard in Maestro 12.4 to improve docking results prior to molecular docking experiments. Unwanted protein chains were removed. The protein structure of tyrosinase was optimized by adding hydrogen atoms, then water molecules were removed and the structure was minimized. The active site of tyrosinase was defined using the co-crystal ligand binding site of the PDB and literature data [55–57]. Compounds 2, 3, and kojic acid were imported to the entry list of Maestro 12.4 in CDXML format and prepared for docking using LigPrep. Molecular docking experiments were performed for compounds 2 and 3 and kojic acid using the Glide docking protocol [58]. Predicted binding energies (docking scores) and binding interactions of ligands within the active region of tyrosinase were obtained using Glide extra precision (XP) [59].

### 4.2.3. Assay of copper-interacting ability [52]

The mixture consisting of 5 μL of a sample compound (2 or 3, 0.05 mM), 5 μL of the aqueous solution of mushroom tyrosinase (139 units), 50 μL of distilled water, and 90 μL of 50 mM phosphate buffer (pH 6.5) with or without CuSO<sub>4</sub> (0.125 mM) was incubated at 37 °C for 30 min, and then the UV–visible spectra (350 – 600 nm) were measured using microplate spectrophotometer (Multiskan GO, Thermo Scientific, CA, USA).

### 4.2.4. Kinetic analysis

Compounds 2 and 3 most potently inhibited mushroom tyrosinase and were selected for the kinetic analysis. The inhibition kinetics of compounds 2 and 3 were investigated using previously reported

methods [56,57] using compound 2 and 3 concentrations of 0, 10, 20, or 40 μM and 0, 7.5, 15, and 30 μM, respectively. L-Tyrosine was used at concentrations of 0, 1, 2, or 4 mM for compound 2 and 0, 2, 4, 8, or 16 mM for compound 3, respectively. Initial rates of dopachrome formation were determined from the initial linear portion of absorbance versus time plots at 10 min intervals up to 50 min after enzyme addition. Inhibition types were determined using Lineweaver-Burk plots of dopachrome formation rate<sup>-1</sup> (1/V) versus substrate concentration<sup>-1</sup> (1/[L-tyrosine] mM<sup>-1</sup>).

### 4.2.5. Cell culture

Murine B16F10 melanoma cells were obtained from the American Type Culture Collection (ATCC, Manassas, VA, USA). Cells were cultured in DMEM (Dulbecco's Modified Eagle Medium) containing 10% FBS (fetal bovine serum), 100 IU/mL penicillin, and 100 μg/mL streptomycin (Gibco/Thermo Fisher Scientific; Carlsbad, CA, USA) in 5% CO<sub>2</sub> humidified atmosphere at 37 °C. The cultured cells were used for subsequent experiments.

### 4.2.6. Viabilities of B16F10 melanoma cells treated with compounds 2 or 3

The EZ-Cytox (EZ-3000, Daeil Lab Service, Seoul, Korea) assay was used to measure cell viabilities after treatment with various concentrations (1, 2, 5, 10, 20, or 50 μM) of compounds 2 or 3 [60]. B16F10 cells were seeded (1 × 10<sup>4</sup> cells/well) in 96 well plates and incubated for 24 h in humidified 5% CO<sub>2</sub> atmosphere at 37 °C. After treatment with test compounds, cells were incubated for an additional 24 h. The next day, the EZ-Cytox reagent was added to cultured cells in a ratio of 1:10 and incubated at 37 °C for 2 h. Cell viabilities were calculated by measuring optical densities at 450 nm. Experiments were conducted independently three times.

### 4.2.7. Cellular tyrosinase activities of B16F10 melanoma cells after treatments of compounds 2 or 3

Cellular tyrosinase inhibitory activities were evaluated by determining the rate of L-DOPA oxidation as previously described with slight modification [61]. B16F10 cells were cultured at a density of 5 × 10<sup>4</sup> cells per well, allowed to attach to the bottom of wells in a 6-well plate, and then incubated overnight in a humidified 5% CO<sub>2</sub> atmosphere at 37 °C. The control and treatment groups were activated with 5 μM α-MSH plus 200 μM IBMX. Cells were treated with test compounds 2 or 3 (final concentrations: 0, 5, 10, or 20 μM) or kojic acid (final concentration: 20 μM) and held for an additional 60 h under standard conditions. Cells were washed 2–3 times with PBS, lysed with lysis buffer (100 μL) (50 mM phosphate buffer (pH 6.5), 0.1 mM phenylmethylsulfonyl fluoride (PMSF), and 1% Triton X-100) and frozen at –80 °C for 30 min. Lysed cells were centrifuged at 12,000 rpm for 30 min at 4 °C, and lysates (80 μL) were incubated with 20 μL of L-dopa (2 mg/mL) at 37 °C for 30 min. Optical densities were measured at 492 nm using a microplate reader (Tecan, Männedorf, Switzerland). Experiments were conducted independently three times.

### 4.2.8. Melanin inhibition by compounds 2 and 3 in B16F10 melanoma cells

Melanin inhibition assays of compounds 2 and 3 in B16F10 cells were performed as previously described with slight modification [62]. B16F10 cells were cultured at a density of 5 × 10<sup>4</sup> cells per well in 6-well plates, allowed to attach, and then incubated overnight in a humidified 5% CO<sub>2</sub> atmosphere at 37 °C. They were then treated with 5 μM α-MSH plus 200 μM IBMX, and compounds 2 and 3 (final concentrations: 0, 5, 10, and 20 μM) or kojic acid (final concentration: 20 μM) were added. Cells were then left for 60 h under standard conditions. For extracellular melanin content, the culture media was directly measured at 405 nm using a microplate reader. For intracellular melanin content, the cell pellets were washed 2–3 times with PBS buffer, treated with 200 μL of 1 N NaOH, and incubated at 60 °C for 1 h to extract the melanin. Melanin absorbances were measured at 405 nm. All results were normalized to the total protein concentration of the cell pellet using a Bicinchoninic

Acid Assay kit (Thermo Fisher Scientific, Inc., MA, USA). Experiments were conducted independently three times.

#### 4.2.9. Statistical analysis

The statistical analysis was conducted using GraphPad Prism (La Jolla, CA, USA). Results are presented as means  $\pm$  standard errors. The significances of intergroup differences were determined using one-way ANOVA and Tukey's test. Statistical significance was accepted for  $p$ -values  $< 0.05$ .

#### Declaration of Competing Interest

The authors declare that they have no known competing financial interests or personal relationships that could have appeared to influence the work reported in this paper.

#### Acknowledgments

This work was supported by a National Research Foundation of Korea (NRF) grant funded by the Korea government (MSIT) (No. NRF-2020R1A2C1004198).

#### Appendix A. Supplementary material

Supplementary data to this article can be found online at <https://doi.org/10.1016/j.bioorg.2021.104688>.

#### References

- Q.-X. Chen, I. Kubo, Kinetics of mushroom tyrosinase inhibition by quercetin, *J. Agric. Food. Chem.* 50 (14) (2002) 4108–4112.
- A.J. Uiterkamp, H.S. Mason, Magnetic dipole-dipole coupled Cu(II) pairs in nitric oxide-treated tyrosinase: a structural relationship between the active sites of tyrosinase and hemocyanin, *PNAS* 70 (4) (1973) 993–996.
- K. Nishioka, Particulate tyrosinase of human malignant melanoma. Solubilization, purification following trypsin treatment, and characterization, *Eur. J. Biochem.* 85 (1) (1978) 137–146.
- A. Sánchez-Ferrer, J. Villalba, F. García-Carmona, Triton $\times$ -114 as a tool for purifying spinach polyphenol oxidase, *Phytochemistry* 28 (5) (1989) 1321–1325.
- H. Raper, The aerobic oxidases, *Physiol. Rev.* 8 (2) (1928) 245–282.
- Olivares, C., et al., The 5, 6-dihydroxyindole-2-carboxylic acid (DHICA) oxidase activity of human tyrosinase. *Biochem. J.*, 2001. 354(1): p. 131–139.
- R. Wang, et al., 2-(4-Fluorophenyl)-quinazolin-4(3H)-one as a novel tyrosinase inhibitor: Synthesis, inhibitory activity, and mechanism, *Bioorg. Med. Chem.* 24 (19) (2016) 4620–4625.
- H. Babich, F. Visioli, In vitro cytotoxicity to human cells in culture of some phenolics from olive oil, *Il Farmaco* 58 (5) (2003) 403–407.
- F. Solano, et al., Hypopigmenting agents: an updated review on biological, chemical and clinical aspects, *Pigment Cell Res.* 19 (6) (2006) 550–571.
- M. Adhikari, et al., Perspective in Pigmentation Disorders, in: *Comprehensive Clinical Plasma Medicine*, Springer, 2018, pp. 363–400.
- Allemann, I.B., Goldberg, D.J. Benign pigmented lesions, in *Basics in Dermatological Laser Applications*. 2011, Karger Publishers. p. 81–96.
- A.J. McEvily, R. Iyengar, W.S. Otwell, Inhibition of enzymatic browning in foods and beverages, *Crit. Rev. Food Sci. Nutr.* 32 (3) (1992) 253–273.
- K. Maeda, M. Fukuda, Arbutin: mechanism of its depigmenting action in human melanocyte culture, *J. Pharmacol. Exp. Ther.* 276 (2) (1996) 765–769.
- B. Fu, et al., Isolation and identification of flavonoids in licorice and a study of their inhibitory effects on tyrosinase, *J. Agric. Food. Chem.* 53 (19) (2005) 7408–7414.
- K.a. Maeda, M. Fukuda, In vitro effectiveness of several whitening cosmetic components in human melanocytes, *J. Soc. Cosmetic Chemists* 42(6) (1991) 361–368.
- E. Frenk, Treatment of melasma with depigmenting agents, *Melasma: New Approac. Treat.* (1995) 9–15.
- M.T. Khan, Novel tyrosinase inhibitors from natural resources - their computational studies, *Curr. Med. Chem.* 19 (14) (2012) 2262–2272.
- K. Bao, et al., Design and synthesis of biphenyl derivatives as mushroom tyrosinase inhibitors, *Bioorg. Med. Chem.* 18 (18) (2010) 6708–6714.
- Y.J. Kim, H. Uyama, Tyrosinase inhibitors from natural and synthetic sources: structure, inhibition mechanism and perspective for the future, *Cell Mol. Life Sci.* 62 (15) (2005) 1707–1723.
- T.-S. Chang, Natural melanogenesis inhibitors acting through the down-regulation of tyrosinase activity, *Materials* 5 (9) (2012) 1661–1685.
- Y. Yuan, et al., Tyrosinase inhibitors as potential antibacterial agents, *Eur. J. Med. Chem.* 187 (2020), 111892.
- I. Cabezedo, et al., Effect directed synthesis of a new tyrosinase inhibitor with anti-browning activity, *Food Chem.* 341 (2021), 128232.
- R.R. Arroo, et al., Flavones as tyrosinase inhibitors: kinetic studies in vitro and in silico, *Phytochem. Anal.* 31 (3) (2020) 314–321.
- Y. Nazir, et al., Hydroxyl substituted benzoic acid/cinnamic acid derivatives: Tyrosinase inhibitory kinetics, anti-melanogenic activity and molecular docking studies, *Bioorg. Med. Chem. Lett.* 30 (1) (2020), 126722.
- M. Mahdavi, et al., Synthesis of new benzimidazole-1,2,3-triazole hybrids as tyrosinase inhibitors, *Chem. Biodivers* 15 (7) (2018), e1800120.
- A. Iraj, et al., Synthesis, biological evaluation and molecular docking analysis of vaniline-benzylidenehydrazine hybrids as potent tyrosinase inhibitors, *BMC Chem.* 14 (1) (2020) 28.
- R. Sara, et al., 6-Methoxy-3,4-dihydronaphthalenone chalcone-like derivatives as potent tyrosinase inhibitors and radical scavengers, *Lett. Drug Des. Discovery* 15 (11) (2018) 1170–1179.
- R. Uchida, S. Ishikawa, H. Tomoda, Inhibition of tyrosinase activity and melanine pigmentation by 2-hydroxytyrosol, *Acta pharmaceutica Sinica. B* 4 (2) (2014) 141–145.
- K. Jimbow, et al., Mechanism of depigmentation by hydroquinone, *J. Invest. Dermatol.* 62 (4) (1974) 436–449.
- Y. Ogiwara, et al., Evaluation of the repeated-dose liver, bone marrow and peripheral blood micronucleus and comet assays using kojic acid, *Mutation Research/Genetic Toxicol. Environ. Mutagenesis* 780 (2015) 111–116.
- W. Westerhof, T. Kooyers, Hydroquinone and its analogues in dermatology – a potential health risk, *J. Cosmet. Dermatol.* 4 (2) (2005) 55–59.
- M. Gaskell, K.I. McLuckie, P.B. Farmer, Genotoxicity of the benzene metabolites para-benzoquinone and hydroquinone, *Chem. Biol. Interact.* 153 (2005) 267–270.
- S.H. Bang, S.J. Han, D.H. Kim, Hydrolysis of arbutin to hydroquinone by human skin bacteria and its effect on antioxidant activity, *J. Cosmet. Dermatol.* 7 (3) (2008) 189–193.
- K. Shimizu, R. Kondo, K. Sakai, Inhibition of tyrosinase by flavonoids, stilbenes and related 4-substituted resorcinols: structure-activity investigations, *Planta Med.* 66 (01) (2000) 11–15.
- Y.M. Ha, et al., Analogs of 5-(substituted benzylidene) hydantoin as inhibitors of tyrosinase and melanin formation, *Biochimica et Biophysica Acta (BBA)-General Subjects* 1810 (6) (2011) 612–619.
- Y.M. Ha, et al., Synthesis and biological activity of hydroxybenzylidene pyrrolidine-2, 5-dione derivatives as new potent inhibitors of tyrosinase, *MedChemComm* 2 (6) (2011) 542–549.
- Chung, K.W., et al., Evaluation of in vitro and in vivo anti-melanogenic activity of a newly synthesized strong tyrosinase inhibitor (E)-3-(2, 4 dihydroxybenzylidene) pyrrolidine-2, 5-dione (3-DBP). *Biochimica et Biophysica Acta (BBA)-General Subjects*, 2012. 1820(7): p. 962–969.
- Y.M. Ha, et al., Design and synthesis of 5-(substituted benzylidene) thiazolidine-2, 4-dione derivatives as novel tyrosinase inhibitors, *Eur. J. Med. Chem.* 49 (2012) 245–252.
- S.H. Kim, et al., Anti-melanogenic effect of (Z)-5-(2, 4-dihydroxybenzylidene) thiazolidine-2, 4-dione, a novel tyrosinase inhibitor, *Arch. Pharmacol. Res.* 36 (10) (2013) 1189–1197.
- H.R. Kim, et al., Benzylidene-linked thiohydantoin derivatives as inhibitors of tyrosinase and melanogenesis: importance of the  $\beta$ -phenyl- $\alpha$ ,  $\beta$ -unsaturated carbonyl functionality, *MedChemComm* 5 (9) (2014) 1410–1417.
- H.J. Jung, et al., A novel synthetic compound, (Z)-5-(3-hydroxy-4-methoxybenzylidene)-2-iminothiazolidin-4-one (MHY773) inhibits mushroom tyrosinase, *Biosci. Biotechnol. Biochem.* 82 (5) (2018) 759–767.
- H.J. Jung, et al., (2E, 5E)-2, 5-Bis (3-hydroxy-4-methoxybenzylidene) cyclopentanone exerts anti-melanogenesis and anti-wrinkle activities in B16F10 melanoma and Hs27 fibroblast cells, *Molecules* 23 (6) (2018) 1415.
- S. Lee, et al., Inhibitory effects of N-(acryloyl) benzamide derivatives on tyrosinase and melanogenesis, *Bioorg. Med. Chem.* 27 (17) (2019) 3929–3937.
- S. Ullah, et al., Tyrosinase inhibition and anti-melanin generation effect of cinnamide analogues, *Bioorg. Chem.* 87 (2019) 43–55.
- S. Ullah, et al., Synthesis of cinnamic amide derivatives and their anti-melanogenic effect in  $\alpha$ -MSH-stimulated B16F10 melanoma cells, *Eur. J. Med. Chem.* 161 (2019) 78–92.
- S. Ullah, et al., Design, synthesis and anti-melanogenic effect of cinnamide derivatives, *Bioorg. Med. Chem.* 26 (21) (2018) 5672–5681.
- E.K. Lee, et al., Tyrosinase inhibitory effect of (E)-2-(substituted benzylidene)-2, 3-dihydro-1H-cyclopenta [a] naphthalen-1-one derivatives, *J. Life Sci.* 27 (2) (2017) 139–148.
- S.J. Kim, et al., The tyrosinase inhibitory effects of isoxazolone derivatives with a (Z)- $\beta$ -phenyl- $\alpha$ ,  $\beta$ -unsaturated carbonyl scaffold, *Bioorg. Med. Chem.* 26 (14) (2018) 3882–3889.
- Oliveira, A.F.C.d.S., et al., Zirconium catalyzed synthesis of 2-arylidene Indan-1,3-diones and evaluation of their inhibitory activity against NS2B-NS3 WNV protease. *Eur. J. Med. Chem.* 2018. 149: p. 98–109.
- M. Tugrak, et al., New azafluorenones with cytotoxic and carbonic anhydrase inhibitory properties: 2-Aryl-4-(4-hydroxyphenyl)-5H-indeno[1,2-b]pyridin-5-ones, *Bioorg. Chem.* 81 (2018) 433–439.
- M. Barge, R. Salunkhe, Aqueous extract of *Balanites roxburghii* fruit: a green dispersant for C-C bond formation, *RSC Adv.* 4 (59) (2014) 31177–31183.
- I. Kubo, et al., Flavonols from heterotheca inuloides: tyrosinase inhibitory activity and structural criteria, *Bioorg. Med. Chem.* 8 (7) (2000) 1749–1755.
- Y.M. Ha, et al., Synthesis and preliminary in vitro biological evaluation of 5-chloro-2-(substituted phenyl)benzo[d]thiazole derivatives designed as novel antimelanogenesis agents, *Appl. Biochem. Biotechnol.* 168 (6) (2012) 1416–1433.

- [54] S.K. Hyun, et al., Inhibitory effects of kurarinol, kuraridinol, and trifolirhizin from *Sophora flavescens* on tyrosinase and melanin synthesis, *Biol. Pharm. Bull.* 31 (1) (2008) 154–158.
- [55] M. Hassan, et al., Exploration of novel human tyrosinase inhibitors by molecular modeling, docking and simulation studies, *Interdiscipl. Sci.: Computat. Life Sci.* 10 (1) (2018) 68–80.
- [56] A. Saeed, et al., Synthesis, molecular docking studies of coumarinyl-pyrazolinyl substituted thiazoles as non-competitive inhibitors of mushroom tyrosinase, *Bioorg. Chem.* 74 (2017) 187–196.
- [57] F.A. Larik, et al., Design, synthesis, kinetic mechanism and molecular docking studies of novel 1-pentanoyl-3-arylthioureas as inhibitors of mushroom tyrosinase and free radical scavengers, *Eur. J. Med. Chem.* 141 (2017) 273–281.
- [58] R.A. Friesner, et al., Extra precision glide: docking and scoring incorporating a model of hydrophobic enclosure for protein–ligand complexes, *J. Med. Chem.* 49 (21) (2006) 6177–6196.
- [59] R. Farid, et al., New insights about HERG blockade obtained from protein modeling, potential energy mapping, and docking studies, *Bioorg. Med. Chem.* 14 (9) (2006) 3160–3173.
- [60] H. Kim, et al., Compound K attenuates stromal cell-derived growth factor 1 (SDF-1)-induced migration of C6 glioma cells, *Nutrit. Res. Pract.* 10 (3) (2016) 259–264.
- [61] S.J. Bae, et al., A novel synthesized tyrosinase inhibitor:(E)-2-((2, 4-dihydroxyphenyl) diazenyl) phenyl 4-methylbenzenesulfonate as an azo-resveratrol analog, *Biosci. Biotechnol. Biochem.* 77 (1) (2013) 65–72.
- [62] L.-G. Chen, et al., Melanogenesis inhibition by gallotannins from Chinese galls in B16 mouse melanoma cells, *Biol. Pharm. Bull.* 32 (8) (2009) 1447–1452.